

ON THE RIEMANN SOLUTIONS OF THE BALANCE EQUATIONS FOR STEAM AND WATER FLOW IN A POROUS MEDIUM*

W. LAMBERT[†], D. MARCHESIN[‡], AND J. BRUINING[§]

Abstract. Conservation laws have been used to model a variety of physical phenomena and therefore the theory for this class of equations is well developed. However, in many problems, such as transport of hot fluids and gases undergoing mass transfer, balance laws are required to describe the flow.

As an example, in this work we obtain the solutions for the basic one-dimensional profiles that appear in the clean up problem or in recovery of geothermal energy. We consider the injection of a mixture of steam and water in several proportions in a porous rock filled with a different mixture of water and steam. We neglect compressibility, heat conductivity and capillarity and present a physical model for steam injection based on the mass balance and energy conservation equations.

We describe completely all possible solutions of the Riemann problem. We find several types of shock between regions and develop a scheme to find the solution from these shocks. A new type of shock, the evaporation shock, is identified in the Riemann solution. This work generalizes the work of Bruining et. al. [2], where the condensation shock appears. It is a step towards obtaining a general method for solving Riemann problems for a wide class of balance equations with phase changes (see [8]).

Key words. Porous medium, steamdrive, Riemann solution, balance equations, multiphase flow

AMS subject classifications. 35L60, 35L67, 76S05

1. Introduction. Professor Joel Smoller has made significant contributions in several mathematical fields, especially in the theory of conservation laws. For several years, the most complete and well written reference in conservation laws and shock theory was the great book “Shock Waves and Reaction-Diffusion Equations” [11]. This book has been the standard reference in conservation laws worldwide for two decades.

In this paper, we use part of the theory developed for conservation laws to solve a system of balance equations for steam and water flow in a porous medium. The solution exhibits an intriguing yet systematic structure. It is desirable to obtain a theory for balance equations as complete as that for conservation laws, (see [8] for an initial discussion); combustion phenomena are also modelled by balance equations, see [1] and references therein.

This class of balance equations has appeared in mathematical models for clean-up, see [2]. Soil and groundwater contamination due to spills of non-aqueous phase liquids (NAPL’s) have received a great deal of attention from society, because, in general, these components can cause damage to the ecosystem and environmental impact to a large area around the spills. Removal of contaminants with steam is considered to be an attractive groundwater remediation technique. We consider here a model for steam injection presented in [2]. Steam injection is widely studied in Petroleum Engineering,

*Received July 1, 2005; accepted for publication February 7, 2006. This work was supported in part by: CNPq scholarship 141573/2002-3, ANP/PRH-32 scholarship, CNPq 301532/2003-6, CNPq 450161/2004-8, FAPERJ E-26/152.163/2002 and IM-AGIMB

[†]Instituto Nacional de Matemática Pura e Aplicada, Estrada Dona Castorina 110, 22460-320 Rio de Janeiro, RJ, Brazil (lambert@fluid.impa.br).

[‡]Instituto de Matemática Pura e Aplicada, Estrada Dona Castorina 110, 22460-320 Rio de Janeiro, RJ, Brazil (marchesi@impa.br).

[§]Dietz Laboratory, Centre of Technical Geoscience, Mijnbouwstraat 120, 2628 RX Delft, The Netherlands (J.Bruining@mp.tudelft.nl).

see [2] and references therein. Steam production from geothermal sources is a related application [3, 12].

We consider the constant rate injection of a mixture of steam/water in a specified proportion into a porous medium filled with another homogeneous steam/water mixture. We study all possible proportions of steam and water as boundary and initial conditions for the problem. We present a physical model for steam injection based on mass balance and energy conservation equations. We present the main physical definitions and equations; we refer to [2] for more details. We study the three possible physical phase mixture situations: single-phase gaseous situation, which represents a region with superheated steam, called steam region, sr ; a two-phase situation, which represents a region where the water and steam coexist called boiling region, br ; and a single-phase liquid situation which represents a region with water only, called water region, wr . We reduce the three balance equations system presented in Sec. 2 to a system of conservation laws that has the following form in each physical situation:

$$\frac{\partial}{\partial t}G(V) + \frac{\partial}{\partial x}uF(V) = 0, \quad (1.1)$$

where $V = (V_1) : \mathbb{R} \times \mathbb{R}^+ \rightarrow \Omega \subset \mathbb{R}$ represents the variables to be determined; $G = (G_1, G_2) : \Omega \rightarrow \mathbb{R}^2$ and $F = (F_1, F_2) : \Omega \rightarrow \mathbb{R}^2$ are the accumulation vector and the flux vector, respectively; $u : \mathbb{R} \times \mathbb{R}^+ \rightarrow \mathbb{R}$, $u = u(x, t)$ is the total velocity. It is useful to define $U = (V, u)$. The vector V represents the water saturation s_w and the temperature T . The state of the system is represented by (s_w, T, u) . Eq. (1.1) has an important feature, the variable u does not appear in the accumulation term, it appears isolated in the flux term, therefore this equation has an infinite speed mode associated to u . Nevertheless we are able to solve the complete Riemann problem associated to Eq. (1.1). Moreover, under certain hypothesis it is possible to solve numerically the problem, in [6] Lambert et. al. consider a model in the balance form for nitrogen and steam injection.

In [2], Bruining et. al. considered as initial condition for the Riemann problem, a porous rock filled with water at a temperature T^0 , in which a mixture of water and steam at saturation temperature (boiling temperature) in given proportions is injected. The main feature was the existence of a Steam Condensation Front (SCF), which is a shock between the br and the wr . The analysis of the shock between each pair of regions is important because bifurcations occur and frequently non-classical structures appear in the solution.

In this work, we completely solve the Riemann problem. We study the three possible physical phase mixture situations: single-phase superheated steam gaseous situation, in the sr ; a two-phase situation where the water and steam coexist in equilibrium in the br ; and a single-phase wr .

The Riemann problem A is the injection of a mixture of water and steam at boiling temperature in a porous rock filled with steam at temperature above the boiling temperature (superheated steam). In this case, a new wave, a vaporization shock (VS), appears between the br and the sr . In the Riemann problem B , we inject liquid water in a porous rock containing water and steam at boiling temperature. These initial and boundary conditions are the reverse of those considered in [2]. There is a water evaporation shock (WES) between the sr and the br . In the Riemann problem C , we inject superheated steam in a porous rock containing water and steam at boiling temperature. There appears a condensation shock (CS) between the sr and the br . This Riemann solution is the most interesting solution; it has a rich bifurcation structure. We obtain two bifurcation curves. The first bifurcation is the TCS locus,

where the left thermal characteristic speed in the sr coincides with the condensation shock speed v^{CS} . The second bifurcation is the CSS locus, where the condensation shock speed v^{CS} coincides with the right saturation characteristic speed λ_g^b in the br . These two bifurcation curves intersect at a point, the double bifurcation SHB (see Fig. 6.2). This state is very important because it is an organizing point between several different phase mixtures. In the Riemann problem D , we inject water at a temperature below its boiling temperature in a porous rock containing superheated steam. There is a br between the wr and the sr . So the Riemann solution consists of a combination of the waves in the Riemann problem B and C . In the Riemann problem E , we inject superheated steam in a porous rock containing water below its boiling temperature. As in the Riemann problem D , there is a br between the wr and the sr . For this Riemann problem, the solution is obtained combining the Riemann solution B and the solution F , see [2] and [5].

In Sec. 2, we present the mathematical and physical formulations of the injection problem in terms of balance equations. In Sec. 3, we consider separately each region in different physical situations under thermodynamic equilibrium and we rewrite the corresponding balance equations in conservative form. In Sec. 4 we study the shock and rarefaction waves that occur in each physical situation separately. In Sec. 5, we study the shocks in the transitions between regions. In Sec. 6, we present the solution of the Riemann problem for the five types of injection. Sec. 7 summarizes our conclusions. In Appendix A, we describe notation and physical quantities appearing in the physical model. The omitted proofs are found in [7].

2. Mathematical and Physical model. We can distinguish a total of five zones in different physical situations in the porous rock: a steam zone at temperature above the boiling temperature, a steam zone at the boiling temperature, a zone containing water and steam at the boiling temperature and a zone containing liquid water at the boiling temperature (all these zones are hot); finally, one zone containing liquid water below the boiling temperature called cold zone.

2.1. The model equations. Ignoring diffusive effects, the mass balance equation for liquid water and steam read:

$$\frac{\partial}{\partial t} \varphi \rho_w s_w + \frac{\partial}{\partial x} \rho_w u_w = +q, \quad (2.1)$$

$$\frac{\partial}{\partial t} \varphi \rho_g s_g + \frac{\partial}{\partial x} \rho_g u_g = -q, \quad (2.2)$$

where φ is the rock porosity assumed to be constant; s_w and s_g are the water and steam saturations; ρ_w is the water density, which is assumed to be constant for simplicity; the steam density ρ_g is a function of the temperature T (i.e, we neglect the effects of gas compressibility) and decreases with temperature; the term q is the mass transfer between the gaseous and liquid water; u_w and u_g are the water and steam phase velocity.

Disregarding heat conductivity, the energy balance equation can be written as:

$$\frac{\partial}{\partial t} \varphi (\hat{H}_r + \rho_w h_w s_w + \rho_g h_g s_g) + \frac{\partial}{\partial x} (u_w \rho_w h_w + u_g \rho_g h_g) = 0, \quad (2.3)$$

where H_r is the rock enthalpy per unit volume and h_w and h_g are the water and gas enthalpies per unit mass, respectively, and $\hat{H}_r = H_r/\varphi$. The enthalpies and ρ_g are functions only of temperature and their expressions are found in Appendix A. From

these expressions, one can see that the enthalpies are increasing functions and that h_g is a convex function.

2.2. Physical Model. To determine the fluid flow rate, we use Darcy's law for multiphase flow without gravity and capillary pressure effects:

$$u_w = -\frac{kk_{rw}}{\mu_w} \frac{\partial p}{\partial x}, \quad u_g = -\frac{kk_{rg}}{\mu_g} \frac{\partial p}{\partial x}, \quad (2.4)$$

where k is the absolute permeability for rock (see Appendix A); the relative permeability functions k_{rw} and k_{rg} are considered to be power functions of their respective effective saturations (see Appendix A); μ_w and μ_g are the viscosity of liquid water and the viscosity of steam and they are functions of temperature; p is the common pressure of the liquid and gaseous phase. We define the fractional flow functions for water and steam depending on the saturation and temperature as follows, see Figure 2.1:

$$f_w = \frac{k_{rw}/\mu_w}{d}, \quad f_g = \frac{k_{rg}/\mu_g}{d} \quad \text{where} \quad d = \frac{k_{rw}}{\mu_w} + \frac{k_{rg}}{\mu_g}. \quad (2.5)$$

Using (2.5) in Darcy's law (2.4)

$$u_w = u f_w, \quad u_g = u f_g, \quad \text{where} \quad u = u_w + u_g, \quad (2.6)$$

and u is the total or Darcy velocity. The saturations s_w and s_g add to 1.

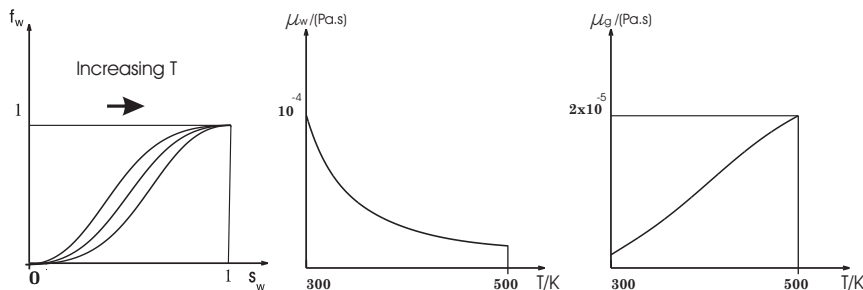


FIG. 2.1. a) Left: The shape of water fractional flux f_w , originating from typical $k_{rw}(s_w)$ and $k_{rg}(s_g)$, given in (A.6) for different values of the temperature T . The separation between the curves is tiny in reality. b) Center: Water viscosity $\mu_w(T)$. c) Right: Gas viscosity $\mu_g(T)$.

3. Regions under thermodynamical equilibrium. As we will see later, the five zones can be organized in three regions in different physical situations where the fluids are in thermodynamic equilibrium, which is often specified by an equation of state (EOS). Each physical situation determines the structure of the governing system of equations. One region consists of steam only, with temperature at least T^b (the condensation temperature of pure water, which is around $373.15K$ at atmospheric temperature), where we must determine two variables: temperature and Darcy velocity u . The steam saturation is $s_g = 1$ ($s_w = 0$). There is a second region consisting of steam and water, with liquid water saturation s_w and gas saturation s_g both less than 1. We must determine two variables: the velocity and saturation (either s_w or s_g , because they add to 1); the temperature here is known and its value is $T = T^b$. Finally there is a region of liquid water, where we must also determine two variables: temperature and velocity. The saturation is known: $s_g = 0$ and $s_w = 1$.

We summarize these regions as follows:

$s_w \setminus T$	$T > T^b$	$T = T^b$	$T < T^b$
$s_w = 0$	superheated steam zone	hot steam zone	3
$s_w < 1$	1	hot steam-water zone	4
$s_w = 1$	2	hot water zone	cold water zone

TABLE 1: Classification according to saturation and temperature.

We call “steam region” (represented by “ sr ”) the superheated steam zone. We call “boiling region” (represented by br) the hot steam zone together with the hot steam-water zone and the hot water zone. We call “water region” (represented by “ wr ”) the hot water zone together with the cold water zone. In [2], there is no region with steam above the boiling temperature; the sr and wr are called “hot region” and “liquid water region” respectively.

Notice that the hot steam zone at boiling temperature belongs to both sr and br ; also, the hot water zone belongs to both br and wr .

REMARK 3.1. *Because of thermodynamical equilibrium, steam cannot exist at temperatures lower than T^b ; similarly, there is no liquid water at a temperature above T^b . Thus the regions with numbers 1-4 in Table 1 do not exist because of our requirement of thermodynamic equilibrium. Regions 1-4 would represent the following unstable mixtures: (1) superheated steam with water, (2) superheated water, (3) steam below T^b and (4) steam-water below T^b .*

3.1. Equations in conservative form. From the previous discussion, we notice that in each region under thermodynamic equilibrium there are two variables to be determined in the system (2.1)-(2.3); the other variables are trivial. For example, in the br the temperature and Darcy speed are determined by the system of equations, but the saturation is trivial, its value is $s_w = 0$. Thus we can rewrite the system (2.1)-(2.3) as a system of two conservation laws and two variables as follows. We add Eq. (2.1) to (2.2) and use (2.6):

$$\frac{\partial}{\partial t} \varphi (\rho_w s_w + \rho_g s_g) + \frac{\partial}{\partial x} u (\rho_w f_w + \rho_g f_g) = 0. \quad (3.1)$$

Using (2.6) in the energy conservation equation (2.3), it becomes:

$$\frac{\partial}{\partial t} \varphi (\hat{H}_r + \rho_w h_w s_w + \rho_g h_g s_g) + \frac{\partial}{\partial x} u (\rho_w h_w f_w + \rho_g h_g f_g) = 0. \quad (3.2)$$

We will use (3.1)-(3.2) from now on. Not only this system models the flow in each region under thermodynamic equilibrium, but it also determines the shocks between regions (see Sec. 5), when supplemented by appropriate thermodynamic equations of state.

As initial conditions, we assume that the porous rock is full of a mixture of water and steam (saturation $s_w(x, t = 0) = s_R$) with constant temperature $T(x, t = 0) = T_R$. As boundary conditions at the injection point at the left of the porous rock, the total injection rate u_L is specified as a constant. The constant water-steam injection ratio needs to be given too, which is (s_L, T_L) . It is specified in terms of the water fractional flow $f_w(s_L, T_L)$ at the injection point.

4. Elementary waves under thermodynamical equilibrium. We consider rarefaction and shocks waves for (3.1)-(3.2) in each region.

4.1. Steam region I-*sr*. The temperature is high, $T > T^b$, so there is only steam, $s_w = 0$, (notice that from Eq. (2.1), $q \equiv 0$) and the state (s_w, T, u) can be represented by $(0, T, u)$. The system (3.1)-(3.2) reduces to

$$\frac{\partial}{\partial t} \varphi \rho_g + \frac{\partial}{\partial x} u \rho_g = 0, \quad (4.1)$$

$$\frac{\partial}{\partial t} \varphi (\hat{H}_r + \rho_g h_g) + \frac{\partial}{\partial x} u \rho_g h_g = 0. \quad (4.2)$$

4.1.1. Rarefaction wave. Assuming that all dependent variables are smooth, we can differentiate (4.1) and (4.2) with respect to their variables:

$$\varphi \rho'_g \frac{\partial T}{\partial t} + u \rho'_g \frac{\partial T}{\partial x} + \rho_g \frac{\partial}{\partial x} u = 0, \quad (4.3)$$

$$\varphi (\hat{H}'_r + C_g) \frac{\partial T}{\partial t} + u C_g \frac{\partial T}{\partial x} + \rho_g h_g \frac{\partial}{\partial x} u = 0, \quad (4.4)$$

where prime denotes derivative relative to T .

We use the notation $\hat{C}_r = \hat{H}'_r = d\hat{H}_r/dT$ for the effective rock heat capacity divided by φ and $C_g = \partial(\rho_g h_g)/\partial T$ for the steam heat capacity per unit volume; we assume that the effective rock heat capacity \hat{C}_r is constant (see Appendix A). We rewrite (4.3)-(4.4) as:

$$B \frac{\partial}{\partial t} \begin{pmatrix} T \\ u \end{pmatrix} + A \frac{\partial}{\partial x} \begin{pmatrix} T \\ u \end{pmatrix} = 0, \quad (4.5)$$

where

$$B = \begin{pmatrix} \varphi \rho'_g & 0 \\ \varphi (\hat{C}_r + C_g) & 0 \end{pmatrix} \quad \text{and} \quad A = \begin{pmatrix} u \rho'_g & \rho_g \\ u C_g & \rho_g h_g \end{pmatrix}. \quad (4.6)$$

The characteristic speed λ and the eigenvector $\vec{r} = (r_1, r_2)^T = (dT, du)^T$ in the following system are the speed of rarefaction waves and the characteristic direction, respectively:

$$\det(A - \lambda B) = 0, \quad A \vec{r} = \lambda B \vec{r}. \quad (4.7)$$

We find only one characteristic speed and vector:

$$\lambda_T^g(T, u) = \frac{u}{\varphi} \frac{\rho_g C_g - \rho'_g \rho_g h_g}{\rho_g (\hat{C}_r + C_g) - \rho'_g \rho_g h_g} = \frac{u}{\varphi} \frac{\rho_g c_g}{\hat{C}_r + \rho_g c_g}, \quad (4.8)$$

$$\text{and } \vec{r}_T = \begin{pmatrix} 1, \\ \frac{u \hat{C}_r}{T(\hat{C}_r + \rho_g c_g)} \end{pmatrix}^T,$$

where $\rho_g = \rho_g(T)$, $h_g = h_g(T)$, $C_g = C_g(T)$, and the derivatives relative to temperature are $\rho'_g = \rho'_g(T)$, $c_g = h'_g(T)$ and \hat{C}_r is constant; we used the equality $\rho'_g = -\rho_g/T$ which follows from Eq. (A.4). The notation for this wave has subscript T because it is a thermal wave; the saturation ($s_w = 0$) stays constant, but the temperature T and

the speed u change. We obtain the thermal rarefaction curve in (T, u) space from \vec{r}_T in (4.9):

$$\frac{du}{dT} = u \frac{\hat{C}_r}{T(\hat{C}_r + \rho_g(T)c_g(T))} \quad \text{or} \quad \frac{du}{u} = \frac{dT}{T \left(1 + \rho_g(T)c_g(T)/\hat{C}_r\right)}. \quad (4.9)$$

The rarefaction wave in the $\{x, t\}$ plane is the solution of the following equations:

$$\left(\frac{dT}{d\xi}, \frac{du}{d\xi}\right)^T = \vec{r}_T, \quad \text{with} \quad \xi = \frac{x}{t} = \lambda_T^g(u(\xi), T(\xi)). \quad (4.10)$$

REMARK 4.1. *In the sr, the temperature decreases from left to right along the thermal rarefaction wave. In the Section 4.1.2 we consider a thermal steam shocks; analogously, on the right of such a shock the temperature is higher than on the left (see [7] and Remark 4.2 for the proofs).*

4.1.2. Thermal steam shock. We assume now that $T^+ > T^- \geq T^b$. Let us consider the thermal discontinuity with speed v_T^g between the $(-)$ state $(0, T^-, u^-)$ and the $(+)$ state $(0, T^+, u^+)$. For such a *thermal steam shock*, Eqs. (4.1)-(4.2) yield the following Rankine-Hugoniot (RH) condition:

$$v_T^g = \frac{u^+ \rho_g^+ - u^- \rho_g^-}{\varphi(\rho_g^+ - \rho_g^-)} = \frac{u^+ \rho_g^+ h_g^+ - u^- \rho_g^- h_g^-}{\varphi\left((\hat{H}_r^+ + \rho_g^+ h_g^+) - (\hat{H}_r^- + \rho_g^- h_g^-)\right)}, \quad (4.11)$$

where $h_g^\pm = h_g(T^\pm)$, $\hat{H}_r^\pm = \hat{H}_r(T^\pm)$ and $\rho_g^\pm = \rho_g(T^\pm)$. From the second equality in Eq. (4.11), we obtain u^+ as a function of u^- :

$$u^+ = u^- \frac{(\hat{H}_r^+ - \hat{H}_r^-)/\rho_g^+ + h_g^+ - h_g^-}{(\hat{H}_r^+ - \hat{H}_r^-)/\rho_g^- + h_g^+ - h_g^-}; \quad (4.12)$$

it is easy to see that the denominator of (4.12) is positive. Moreover $u^+ > u^-$.

We substitute (4.12) in Eq. (4.11); since u^+ is function of u^- , we obtain $v_T^g = v_T^g(T^-, u^-; T^+)$ or $v_T^g = v_T^g(T^-; T^+, u^+)$:

$$v_T^g = \frac{u^-}{\varphi} \frac{h_g^+ - h_g^-}{(\hat{H}_r^+ - \hat{H}_r^-)/\rho_g^- + h_g^+ - h_g^-} = \frac{u^+}{\varphi} \frac{h_g^+ - h_g^-}{(\hat{H}_r^+ - \hat{H}_r^-)/\rho_g^+ + h_g^+ - h_g^-}. \quad (4.13)$$

REMARK 4.2. *Notice that we can rewrite (4.13.a) as:*

$$v_T^g = v_T^g(T^-, u^-; T^+) = \frac{u^-}{\varphi} \frac{(\hat{C}_r/\rho_g^- + (h_g^+ - h_g^-)/(T^+ - T^-))}{\hat{C}_r/\rho_g^- + (h_g^+ - h_g^-)/(T^+ - T^-)}.$$

Defining $\lambda_g^\pm = \lambda_T^g(T^\pm, u^\pm)$, from convexity of $h_g(T)$ it follows that $v_T^g < \lambda_g^-$ for $T^+ > T^-$. Using (4.13.b) we see that $\lambda_g^+ < v_T^g < \lambda_g^-$ if $T^+ > T^-$, so the steam shock satisfies the Lax condition. The equality $v_T^g = \lambda_g^-$ holds if, only if, $T^+ = T^-$.

4.2. Boiling region II - br. Because the temperature is constant and equal to the boiling temperature T^b it can be shown (see [2]), that there is no mass exchange between phases and that the system (3.1)-(3.2) reduces to a single scalar equation with fixed $u = u^b$:

$$\varphi \frac{\partial}{\partial t} s_w + u^b \frac{\partial}{\partial x} f_w = 0. \tag{4.14}$$

Eq. (4.14) supports classical Buckley-Leverett rarefaction and shock waves.

4.2.1. Saturation shocks. Consider a (-) state (s_w^-, T^b, u^b) and a (+) state (s_w^+, T^b, u^b) ; we obtain the following RH condition, where u^b is the common Darcy velocity, $T = T^b$ and we use the nomenclature $f_w^b(s_w) = f_w(s_w, T^b)$:

$$v_s^b(s_w^-, u^b; s_w^+) = v_s(s_w^-, T^b, u^b; s_w^+) = \frac{u^b}{\varphi} \frac{f_w^b(s_w^+) - f_w^b(s_w^-)}{s_w^+ - s_w^-} = \frac{u^b}{\varphi} \frac{f_g^b(s_g^+) - f_g^b(s_g^-)}{s_g^+ - s_g^-}. \tag{4.15}$$

A particular shock for (4.14) separates a mixture of steam and water on the left from pure water on the right, both at boiling temperature. Following [2] we call it the *Hot Isothermal Steam-Water shock* (or *HISW*) between the (-) state (s_w^-, T^b, u^b) and the (+) state $(s_w^+ = 1, T^b, u^b)$. It has speed $v_{g,w}^b$ given by:

$$v_{g,w}^b(s_w^-, u^b) = v_{g,w}(s_w^-, T^b, u^b) = \frac{u^b}{\varphi} \frac{1 - f_w^b(s_w^-)}{1 - s_w^-} = \frac{u^b}{\varphi} \frac{f_g^b(s_g^-)}{s_g^-}. \tag{4.16}$$

Another particular shock for (4.14) separates pure water on the left from a mixture of steam and water on the right, both at boiling temperature. We call it the *Hot Isothermal Water-Steam shock* (or *HIWS*) between the (-) state (s_w^-, T^b, u^b) and the (+) state $(s_w^+ = 0, T^b, u^b)$. It has speed $v_{g,s}^b$ given by

$$v_{g,s}^b(s_w^-, u^b) = v_{g,s}(s_w^-, T^b, u^b) = \frac{u^b}{\varphi} \frac{f_w^b(s_w^-)}{s_w^-}. \tag{4.17}$$

Notice that $v_{g,s}(s_w = 0, T^b, u^b) = v_{g,w}(s_w = 1, T^b, u^b) = 0$.

4.2.2. Saturation rarefaction waves. We will denote by λ_s^b the speed of propagation of saturation waves in the *br*. It is obtained from Eq. (4.14) as:

$$\lambda_s^b = \lambda_s(s_w, T^b, u^b) = \frac{u^b}{\varphi} \frac{\partial f_w^b}{\partial s_w}(s_w). \tag{4.18}$$

4.3. Water region - wr. The system (3.1)-(3.2) reduces to a scalar equation, with constant u^w and $s_w = 1$:

$$\varphi \frac{\partial}{\partial t} \left(\hat{H}_r(T) + \rho_w h_w(T) \right) + u^w \frac{\partial}{\partial x} \rho_w h_w(T) = 0. \tag{4.19}$$

Between a (-) state $(1, T^-, u^w)$ and a (+) state $(1, T, u^w)$, the following RH condition for the thermal discontinuity is valid:

$$v_T^w = \frac{u^w}{\varphi} \frac{\rho_w (h_w - h_w^-)}{\hat{H}_r + \rho_w h_w - (\hat{H}_r^- + \rho_w h_w^-)} = \frac{u^w}{\varphi} \frac{C_w}{\hat{C}_r + C_w}, \tag{4.20}$$

where u^w is Darcy speed in the *wr* and $C_w = \rho_w \partial h_w / \partial T$; the second equality is obtained taking into account (A.5). If $T^- = T^b$ or $T = T^b$, then $u^b = u^w$. From (4.20), the discontinuity is a contact wave and there is no other characteristic speed in this region.

5. Shocks between regions. Within shocks separating regions there is no thermodynamic equilibrium, so q is not zero; however we can still use the system (3.1)-(3.2), because in each region the number of variable to be determined in the system (2.1)-(2.3) is at most 2. This system contains another variable, namely the mass transfer term q . However this variable is not essential to obtain the Riemann solution. It is useful to define the cumulative mass transfer function:

$$\mathcal{Q}(x, t) = \int^x q(\xi, t) d\xi, \tag{5.1}$$

where this integral should be understood in the distribution sense. From Eq. (5.1), we can write $q = \partial\mathcal{Q}(x, t)/\partial x$.

We also define $\mathcal{Q}^-(t) = \mathcal{Q}(x^-, t)$ and $\mathcal{Q}^+(t) = \mathcal{Q}(x^+, t)$, where x^- and x^+ are the points immediately on the left and right of the transition between regions. We define the accumulative balance as the difference between $\mathcal{Q}^+(t)$ and $\mathcal{Q}^-(t)$ and denote it by $[\mathcal{Q}]$.

We can rewrite the system (2.1)-(2.3) (in distribution sense) as:

$$\frac{\partial}{\partial t} G(s_w, T) + \frac{\partial}{\partial x} (uF(s_w, T) - Q(s_w, T)) = 0, \tag{5.2}$$

where $Q = (\mathcal{Q}(V), -\mathcal{Q}(V), 0)^T$; $G = (G_1, G_2, G_3)^T$ and $F = (F_1, F_2, F_3)^T$. The components of F and G are readily obtained from Eqs. (2.1)-(2.3) using (2.6).

The shock waves are discontinuous solutions of Eq. (5.2) and satisfy the RH condition:

$$s(G(s_w^+, T^+) - G(s_w^-, T^-)) = u^+ F(s_w^+, T^+) - u^- F(s_w^-, T^-) - [\mathcal{Q}], \tag{5.3}$$

The problem studied in this paper is an example of the global formalism proposed in [8], where we study better the concept of shock between regions.

5.1. Water Evaporation Shock. WES - This is the discontinuity between a $(-)$ state $(1, T^-, u^-)$ in the wr and a $(+)$ state (s_w^+, T^b, u^+) in the br . It satisfies the following RH conditions for the speed v^{WES} , obtained from Eqs. (3.1)-(3.2):

$$u^+ (\rho_w f_w^+ + \rho_g^b f_g^+) - \varphi v^{WES} (\rho_w s_w^+ + \rho_g^b s_g^+) = u^- \rho_w - \varphi v^{WES} \rho_w, \tag{5.4}$$

$$\begin{aligned} & u^+ (\rho_w h_w^b f_w^+ + \rho_g^b h_g^b f_g^+) - u^- \rho_w h_w^- \\ & = v^{WES} \varphi \left(\hat{H}_r^b + \rho_w h_w^b s_w^+ + \rho_g^b h_g^b s_g^+ - \hat{H}_r^- - \rho_w h_w^- \right). \end{aligned} \tag{5.5}$$

where $f_w(s_w = 1, \cdot) = 1$, $f_w^+ = f_w(s_w^+, T^b)$ and $f_g = 1 - f_w$.

The Darcy speed u^+ is found from u^- using (5.4) and (5.5) as:

$$u^+ = u^- \frac{(\hat{H}_r^b - \hat{H}_r^-) + s_w^+ \rho_w (h_w^b - h_w^-) + s_g^+ \rho_g^b (h_g^b - h_w^-)}{(\hat{H}_r^b - \hat{H}_r^-) \left(f_g^+ \left(\rho_g^b / \rho_w \right) + f_w^+ \right) + \left(\rho_g^b (s_w^+ - f_w^+) + \rho_w f_w^+ \right) (h_w^b - h_w^-) + s_g^+ \rho_g^b (h_g^b - h_w^-)}. \tag{5.6}$$

Eq (5.6) is always valid because $T^- < T^b$, so each term in the denominator is positive. The terms $\hat{H}_r^b - \hat{H}_r^-$ and $h_w^b - h_w^-$ are positive because the enthalpies increase with temperature. The term $h_g^b - h_w^-$ is positive because $h_g^b > h_w^b$ and since $h_w^b > h_w^-$ the positivity follows.

Since we can write u^+ as function of u^w , we obtain $v^{WES} = v^{WES}(T^-, u^-; s_w^+)$:

$$v^{WES} = \frac{u^+}{\varphi} \frac{f_g^+ \rho_g^b (h_g^b - h_w^-) + f_w^+ \rho_w (h_w^b - h_w^-)}{\hat{H}_r^b - \hat{H}_r^- + s_g^+ \rho_g^b (h_g^b - h_w^-) + s_w^+ \rho_w (h_w^b - h_w^-)}. \quad (5.7)$$

The denominator of v^{WES} in (5.7) is never zero because each term in the sum is positive.

LEMMA 5.1. *Define $\mathcal{L}(T)$ as:*

$$\mathcal{L}(T) = \rho_g^b (h_g^b - h_w^T) - \rho_w (h_w^b - h_w^T), \quad (5.8)$$

where $h_w^T = h_w(T)$. There is a unique temperature $T^\dagger < T^b$ such that $\mathcal{L}(T^\dagger) = 0$. Moreover, $\mathcal{L}(T) < 0$ for $T < T^\dagger$ and $\mathcal{L}(T) > 0$ for $T > T^\dagger$.

Substituting $s_g^+ = 1 - s_w^+$, $f_g^+ = 1 - f_w^+$, using Lemma 5.1 for $T \neq T^\dagger$, we rewrite Eq. (5.7)

$$v^{WES} = \frac{u^+}{\varphi} \frac{f_w^+ - f_w^{WES}}{s_w^+ - s_w^{WES}}, \quad f_w^{WES} \equiv \frac{\rho_g^b (h_g^b - h_w^-)}{\mathcal{L}(T^-)}, \quad s_w^{WES} \equiv \frac{\hat{H}_r^b - \hat{H}_r^- + \rho_g^b (h_g^b - h_w^-)}{\mathcal{L}(T^-)}, \quad (5.9)$$

Eqs. (5.9) are the basis for a graphical construction of the WES, see Fig. 6.1.b.

For $T^- < T^\dagger$, f_w^{WES} and s_w^{WES} are negative, while for $T^- > T^\dagger$, $f_w^{WES} > 1$ and $s_w^{WES} > 1$. When $T^- = T^\dagger$, we obtain that $\rho_g^b (h_g^b - h_w^-) = \rho_w (h_w^b - h_w^-)$, so Eq. (5.7) reduces to:

$$v^{WES}(1, T^- = T^\dagger, u^w; s_w^+) = \frac{u^+}{\varphi} \frac{\rho_w (h_w^b - h_w^\dagger) (f_w^b + f_g^b)}{\hat{H}_r^b - H_r^\dagger + \rho_w (h_w^b - h_w^\dagger) (s_w + s_g)} = \frac{u^-}{\varphi} \frac{C_w}{\hat{C}_r + C_w}. \quad (5.10)$$

Notice that if $u^- = u^+$, $v^{WES} = v_T^w$ in the wr , see Eq (4.20).

5.2. Vaporization Shock. VS - It is a discontinuity between a $(-)$ state (s_w^-, T^b, u^-) in the br and a $(+)$ state $(0, T^+ > T^b, u^+)$ in the sr . The Vaporization Shock satisfies the following RH conditions with speed v^{VS} obtained from Eqs. (3.1)-(3.2):

$$v^{VS} \varphi (\rho_g^+ - \rho_g^b s_g^- - \rho_w s_w^-) = u^+ \rho_g^+ - u^- (\rho_w f_w^- + \rho_g^b f_g^-), \quad (5.11)$$

$$v^{VS} \varphi (H_r^+ - H_r^b + \rho_g^+ h_g^+ - s_g^- \rho_g^b h_g^b - s_w^- \rho_w h_w^b) = u^+ \rho_g^+ h_g^+ - u^- (\rho_g^b h_g^b f_g^- + \rho_w h_w^b f_w^-), \quad (5.12)$$

where $h_g^+ = h_g(T^+)$, $h_w^+ = h_w(T^+)$, $H_r^+ = H_r(T^+)$, $\rho_g^+ = \rho_g(T^+)$ and $f_w^- = f_w(s_w^-, T^b)$.

Since $T > T^b$, we obtain v^{VS} as the following fraction, which has positive denominator:

$$v^{VS} = v^{VS}(s_w^-, u^-; T^+) = \frac{u^-}{\varphi} \frac{f_g^- \rho_g^b (h_g^+ - h_g^b) + f_w^- \rho_w (h_w^+ - h_w^b)}{\hat{H}_r^+ - \hat{H}_r^b + s_g^- \rho_g^b (h_g^+ - h_g^b) + s_w^- \rho_w (h_w^+ - h_w^b)}. \quad (5.13)$$

We rewrite Eq. (5.13) in a shorter form. Substituting $s_g = 1 - s_w$ and $f_g = 1 - f_w$, we define $\mathbb{A}(T^+) = \rho_g^b (h_g^+ - h_g^b) - \rho_w (h_w^+ - h_w^b)$. For $T^+ > T^b$ one proves that $\mathbb{A} < 0$.

We multiply and divide (5.13) by \mathbb{A} and we obtain:

$$v^{VS} = \frac{u^- f_w^- - f_w^{VS}}{\varphi s_w^- - s_w^{VS}}, \tag{5.14}$$

$$\text{where } f_w^{VS} \equiv \frac{\rho_w (h_g^+ - h_w^b)}{\mathbb{A}(T^+)}, \quad s_w^{VS} \equiv \frac{\hat{H}_r^+ - \hat{H}_r^b + \rho_g^b (h_g^+ - h_w^b)}{\mathbb{A}(T^+)};$$

notice that f_w^{VS} and s_w^{VS} are negative. Eqs. (5.14) are the basis for a graphical construction of VS , see Fig. 6.1.a.

The Darcy speed u^+ in the sr is the fraction with positive denominator:

$$u^+ = u^- \frac{A^+(\rho_w(s_g^- - f_g^-) + \rho_g^+ f_g^-) + B^+(\rho_g^b(s_w^- - f_w^-) + f_w^- \rho_g^+) + C^+(f_g^- \rho_g^b + f_w^- \rho_w)}{(A^+ s_g^- + B^+ s_w^- + C^+) \rho_g^+}, \tag{5.15}$$

where:

$$A^+ = \rho_g^b (h_g^+ - h_w^b), \quad B^+ = \rho_w (h_g^+ - h_w^b), \quad C^+ = \hat{H}_r^+ - \hat{H}_r^b. \tag{5.16}$$

5.3. Condensation Shock. CS - This is the discontinuity between a $(-)$ state $(0, T^- > T^b, u^-)$ in the sr and a $(+)$ state (s_w^+, T^b, u^+) in the br . It is the reverse of the shock VS . From (5.15):

$$u^+ = u^- \frac{(A^- s_g^+ + B^- s_w^+ + C^-) \rho_g^-}{A^-(\rho_w(s_g^+ - f_g^+) + \rho_g^- f_g^+) + B^-(\rho_g^b(s_w^+ - f_w^+) + f_w^+ \rho_g^-) + C^-(f_g^+ \rho_g^b + f_w^+ \rho_w)}, \tag{5.17}$$

A^- , B^- and C^- are obtained from A^+ , B^+ and C^+ in (5.16) by substituting T^+ by T^- .

Since the CS is reverse of the VS and u^+ is a function of u^- , we obtain $v^{CS} = v^{CS}(T^-, u^-; s_w^+)$:

$$v^{CS} = \frac{u^+}{\varphi} \frac{f_g^+ \rho_g^b (h_g^- - h_w^b) + f_w^+ \rho_w (h_g^- - h_w^b)}{\hat{H}_r^- - \hat{H}_r^b + s_g^+ \rho_g^b (h_g^- - h_w^b) + s_w^+ \rho_w (h_g^- - h_w^b)} \quad \text{or} \quad v^{CS} = \frac{u^+ f_w^+ - f_w^{CS}}{\varphi s_w^+ - s_w^{CS}}. \tag{5.18}$$

Since the CS shock is reverse of the VS , f_w^{CS} and s_w^{CS} are obtained from f_w^{VS} and s_w^{VS} in (5.14) by substituting T^+ by T^- ; notice that the denominator in (5.18.a) is never zero.

5.4. Steam condensation front. SCF - This is the discontinuity between a $(-)$ state $(s_w^- < 1, T^b, u^-)$ in the br and a $(+)$ state $(1, T^+, u^+)$ in the wr . It is the reverse of the WES, so $v^{SCF} = v^{SCF}(s_w^-, u^-; T^+)$ is given by:

$$v^{SCF} = \frac{u^-}{\varphi} \frac{f_g^- \rho_g^b (h_g^b - h_w^+) + f_w^- \rho_w (h_w^b - h_w^+)}{\hat{H}_r^b - \hat{H}_r^+ + s_g^- \rho_g^b (h_g^b - h_w^+) + s_w^- \rho_w (h_w^b - h_w^+)} = \frac{u^- f_w^- - f_w^{SCF}}{\varphi s_w^- - s_w^{SCF}}. \tag{5.19}$$

Here (5.19) is derived as Eq. (5.9), with f_w^{SCF} and s_w^{SCF} obtained from f_w^{WES} and s_w^{WES} in (5.9) by substituting T^+ by T^- .

From Eqs. (5.4)-(5.5), we can find u^+ as the following fraction with positive denominator:

$$u^+ = u^- \frac{(\hat{H}_r^b - \hat{H}_r^+)(f_g^- (\rho_g^b/\rho_w) + f_w^-) + (\rho_g^b(s_w^- - f_w^-) + \rho_w f_w^-) (h_w^b - h_w^+) + s_g^- \rho_g^b (h_g^b - h_w^+)}{\hat{H}_r^b - \hat{H}_r^+ + s_w^- \rho_w (h_w^b - h_w^+) + s_g^- \rho_g^b (h_g^b - h_w^+)}. \tag{5.20}$$

6. The Riemann Solution. The Riemann problem is the solution of (3.1)-(3.2) with initial data

$$\begin{cases} L = (s_L, T_L, u_L) & \text{if } x > 0 \\ R = (s_R, T_R, \cdot) & \text{if } x < 0, \end{cases} \tag{6.1}$$

where $s := s_w$ is the water saturation. We will see that the speed u cannot be prescribed on both sides. Given a speed on one side the other one is obtained by solving the system (2.1)-(2.3); in this case we have chosen to prescribe u_L .

We consider in this paper the Riemann problem for all initial data; we divide the data as follows (the Riemann problem with Data F was solved in [2]):

Riemann Problem	L state	R state
Data A	Steam and Water, $T_L = T^b$	Steam, $T_R > T^b$
Data B	Water, $T_L < T^b$	Steam and Water, $T_R = T^b$
Data C	Steam, $T_L > T^b$	Steam and Water, $T_R = T^b$
Data D	Water, $T_L < T^b$	Steam, $T_R > T^b$
Data E	Steam, $T_L > T^b$	Water, $T_R < T^b$
Data F	Steam and water, $T_L = T^b$	Water, $T_R < T^b$

6.1. Wave Sequences and Riemann Solution. A Riemann solution is a sequence of elementary waves w_k for $k = 1, 2, \dots, m$ (shocks and rarefactions) and constant states U_k for $k = 1, 2, \dots, m$.

$$U_L \equiv U_0 \xrightarrow{w_1} U_1 \xrightarrow{w_2} \dots \xrightarrow{w_m} U_m \equiv U_R. \tag{6.2}$$

We represent any state (s, T, u) by U . The wave w_k has left and right states U_{k-1} and U_k and speeds $\xi_k^- < \xi_k^+$ in case of rarefaction waves and $v = \xi_k^- = \xi_k^+$ in case of shock waves. The left state of the first wave w_1 is (s_L, T_L, u_L) and the right state of w_m is (s_R, T_R, u_R) , where u_R needs to be found. In the Riemann solution it is necessary that $\xi_k^+ \leq \xi_{k+1}^-$; this inequality is called *geometrical compatibility*. When $\xi_k^+ < \xi_{k+1}^-$ there is a separating constant state U_{k+1} between w_k and w_{k+1} ; in this sequence the wave w_k is indicated by \mapsto . If $\xi_k^+ = \xi_{k+1}^-$ there is no actual constant state in physical space, so the wave w_k is a composite with w_{k+1} in this sequence; it is indicated by \mapsto .

Different physical situations are separated by shocks respecting the geometrical compatibility. Sometimes it is useful to emphasize the waves in the sequence (6.2) and not the states. In such cases we use the notation:

$$w_1 \mapsto w_2 \mapsto \dots \mapsto w_m, \tag{6.3}$$

where for each w_k , \mapsto stands for \mapsto for $\xi_k^+ < \xi_{k+1}^-$ and \mapsto for $\xi_k^+ = \xi_{k+1}^-$.

The rarefaction waves are denoted by R_T for thermal rarefactions in sr and R_s for (Buckley-Leverett) saturation rarefactions in br . The shocks in regions under thermodynamic equilibrium are denoted with a single subscript, S_T for thermal shocks in sr , S_s for (Buckley-Leverett) saturation shocks, S_G for HIWS in br and S_W for thermal discontinuities in wr . We recall that the shocks between regions are WES , VS , CS and SCF .

6.2. Riemann Problem A.

6.2.1. Water injection. First, we inject water with temperature T^b , i.e., $L = (1, T^b, u_L)$ in a porous rock filled with superheated steam, i.e., $R = (0, T_R > T^b, u_R)$, which is a sr . In the br , generated by the L state, the flow is governed by a Buckley-Leverett equation. It is well known that the Buckley-Leverett rarefaction has speed λ_s^b given by (4.18) from $s_w = 1$ to $s_w = s^*$, which is defined by:

$$\frac{\partial f_w}{\partial s_w}(s^*, T^b) = \frac{f_w(s^*, T^b)}{s^*}. \tag{6.4}$$

There is a saturation shock and the solution is continued by a shock in the br .

Since the temperature increases in the rarefaction joining the $(-)$ state $(0, T^b, u^-)$ to the $(+)$ state $(0, T^+ > T^b, u^+)$, see Rem. 4.1, there is a shock with speed v_T^g given by (4.13).

LEMMA 6.1. *The speed $v_{g,s}^b$ of the HIWS shock between (s^*, T^b, u^-) and $(0, T^b, u = u^-)$ given by (4.17) is larger than the speed v_T^g of the shock between $(0, T^b, u^-)$ and $(0, T > T^b, u^+)$.*

Thus we conclude that there is a shock with speed v^{VS} between the br and the sr . Let f_w^{VS} and s_w^{VS} be given by (5.14); from the Sec. 6.1, we find a saturation $\hat{s} > s^*$ defined by the following equality, (Fig. 6.1.a):

$$v^{VS}(\hat{s}) = \frac{u^b f_w(\hat{s}, T^b) - f_w^{VS}}{\varphi \hat{s} - s_w^{VS}} = \frac{u^b}{\varphi} \frac{\partial f_w}{\partial s_w}(\hat{s}, T^b). \tag{6.5}$$

PROPOSITION 6.1. *There are two saturation values that satisfy (6.5) for each $T^+ > T^b$. The largest value satisfies (6.5) and maximizes v^{VS} while the other minimizes v^{VS} ; because of geometrical compatibility, we choose the largest value and we denote it by \hat{s} . It is called ‘‘Hot-Bifurcation saturation I’’ or HBI.*

Proof. Geometrically, Eq. (6.5) represents tangency points of the secant from the point (s_w^{VS}, f_w^{VS}) to the graph f_w for each fixed T^+ (Fig. 6.1.a). See [7] for an analytical proof. \square

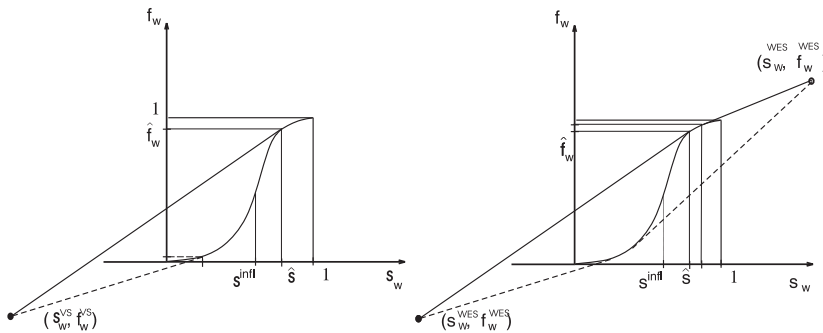


FIG. 6.1. a) Left: Coincidence between v^{VS} and λ_s^b . The largest water saturation maximizes v^{VS} and the other minimizes v^{VS} . b) Right: We represent two possible points (s_w^{WES}, f_w^{WES}) . If $T^- < T^\dagger$ (T^\dagger is defined in Lemma 5.1), both s_w^{WES} and f_w^{WES} are negative; otherwise both are larger than 1.

It is necessary that $v^{VS}(\hat{s}) > v_T^g$; otherwise, the geometrical compatibility in Sec. 6.1 says that the vaporization shock VS does not exist. This is summarized as follows:

LEMMA 6.2. *The vaporization shock between $(-)$ state (s_w^-, T^b, u^-) and $(+)$ state $(1, T^+, u^+)$ with speed v^{VS} given by (5.13) is larger than v_T^g for $s^* \leq s_w^- \leq 1$ and $T^+ > T^b$. (We recall that s^* is defined in Eq. (6.4)).*

From (4.17), we conclude that $v_{g,s}^b$ and s_w decrease together. From (4.13), v_T^g is constant. So we expect that there is a saturation s^{**} where $v_T^g = v_{g,s}^b(s^{**}, s_w = 0)$, which is called ‘‘Hot-Bifurcation II saturation’’, or HBII. One can verify the following:

PROPOSITION 6.2. *For each fixed T^+ , there is a unique saturation s^{**} for which*

$$v_T^g(T^b, u^-; T^+) = v_{g,s}^b(u^-; s^{**}) = v^{VS}(s^{**}, u^-; T^+). \tag{6.6}$$

Furthermore s^{**} is defined in terms of T^+ by any of the following equivalent equalities:

1. $v_T^g(T^b, u^-; T^+) = v_{g,s}^b(u^-; s^{**})$;
2. $v_{g,s}^b(u^-; s^{**}) = v^{VS}(s^{**}, u^-; T^+)$;
3. $v_T^g(T^b, u^-; T^+) = v^{VS}(s^{**}, u^-; T^+)$.

See [8] for a more general result.

LEMMA 6.3. *For any $T^+ > T^b$, the saturation s^{**} given by Eq. (6.6) satisfies $s^{**} < \hat{s}$.*

Solution. Now we can describe the possible solutions for Riemann Data A :

For $\hat{s} \leq s_L \leq 1$. The waves $R_s \rightarrow VS$, with \hat{s} given by Eq. (6.5) and the sequence:

$$L = (s_L, T^b, u_L) \xrightarrow{R_s} (\hat{s}, T^b, u_L) \xrightarrow{VS} (0, T_R, u_R) = R. \tag{6.7}$$

For $s^{} \leq s_L < \hat{s}$.** The wave VS with s^{**} given by Eq. (6.6) and the sequence:

$$L = (s_L, T^b, u_L) \xrightarrow{VS} (0, T_R, u_R) = R. \tag{6.8}$$

For $s_L < s^{}$.** The waves $S_G \mapsto S_T$, with sequence:

$$(s_L, T^b, u_L) \xrightarrow{S_G} (0, T^b, u_L) \xrightarrow{S_T} (0, T_R, u_R). \tag{6.9}$$

6.3. Riemann Problem B. Since the flow in the wr is governed by the linear Eq. (4.19) with constant characteristic speed v_T^w given by (4.20), this wave is a contact discontinuity.

For the Riemann problem $L = (1, T_L \leq T^b, u_L)$ and $R = (s_R, T^b, u_R)$, we have the following:

PROPOSITION 6.3. *For each $(-)$ state $(1, T^- < T^b, u^-)$ and $(+)$ state (s_w^+, T^+, u^+) , there is a water saturation $s^b = s^b(T^-)$, such that for s_w^+ satisfying $s^b \leq s_w^+ \leq 1$, the shock speeds v^{WES} and v_T^w satisfy:*

$$v_T^w \geq v^{WES}, \quad s^b \leq s_w^+ \leq 1; \tag{6.10}$$

the equality occurs only if $s_w^+ = 1$ or $s_w^+ = s^b$. We call s^b a ‘‘Cold Bifurcation saturation I’’ or CBI. Moreover, there is a water saturation $s_{\dagger\dagger} = s_{\dagger\dagger}(T^-)$ satisfying $s^b < s_{\dagger\dagger}$ such that:

$$\lambda_s^b(s_{\dagger\dagger}) = v^{WES}(T^-, u^-; s_{\dagger\dagger}). \tag{6.11}$$

In the nomenclature of [4], the state $s_w = 1$ is the left-extension of $s_{\dagger\dagger}$ with speed λ_s^b . Also, $s_{\dagger\dagger}$ here coincides with $s_{\dagger\dagger}$ obtained in [2]. This saturation maximizes v^{WES} (and consequently v^{SCF}); we call $s_{\dagger\dagger}$ the ‘‘Cold Bifurcation saturation II’’ or CBII.

REMARK 6.1. Notice that from Sec. 5.1, f_w^{WES} and s_w^{WES} are negative if $T^- < T^\dagger$ and positive if $T^- > T^\dagger$ (see Fig. 6.1.b). The solution behavior is the same in both cases.

Prop. 6.3 yields the following Corollaries used to obtain the solution in the br :

COROLLARY 6.1. If $s^{infl}(T^b) < s_w^+ < s_{\dagger\dagger}$, the solution continues in the br as a rarefaction to s_w^+ . If $s_w^+ < s^{infl}$ the rarefaction continues to s^\S , where s^\S is defined by the second equality in:

$$v^{\S,+} = \frac{\partial f_w}{\partial s_w}(s^\S, T^b) = \frac{f_w(s_w^+, T^b) - f_w(s^\S, T^b)}{s_w^+ - s^\S}, \quad (6.12)$$

where $s^{infl} = s^{infl}(T^b)$ is the inflection saturation defined by:

$$\left. \frac{\partial^2}{\partial s_w^2} f_w(s_w, T^b) \right|_{s_w = s^{infl}} = 0. \quad (6.13)$$

COROLLARY 6.2. As the left state temperature T^- tends to the water boiling temperature, the water saturation $s_{\dagger\dagger}$ tends to 1, i.e., the limit of $s_{\dagger\dagger}$ lies in the wr .

Solution. Now we can describe the possible solutions for Riemann Data B:

For $s_R > s_{\dagger\dagger}$. As $s_{\dagger\dagger}$ satisfies (6.11), $(u^b/\varphi)\partial f_w(s_R, T^b)/\partial s_w < v^{WES}$, i.e, the shock v^{WES} is faster than the characteristic speed in the br , the wave sequence is:

$$L = (1, T_L, u_L) \xrightarrow{WES} (s_R, T^b, u_R) = R. \quad (6.14)$$

For $s^{infl}(T^b) < s_R < s_{\dagger\dagger}$. The waves $WES \rightarrow R_s$, with sequence:

$$L = (1, T_L, u_L) \xrightarrow{WES} (s_{\dagger\dagger}, T^b, u_R) \xrightarrow{R_s} (s_R, T^b, u_R) = R. \quad (6.15)$$

For $s_R < s^{infl}(T^b)$. The waves $WES \rightarrow R_s \rightarrow S_s$ with sequence:

$$L = (1, T_L, u_L) \xrightarrow{WES} (s_{\dagger\dagger}, T^b, u_R) \xrightarrow{R_s} (s^\S, T^b, u_R) \xrightarrow{S_s} (s_R, T^b, u_R) = R, \quad (6.16)$$

where s^\S is given by Eq. (6.12).

6.4. Riemann Problem C. Let $L = (0, T_L > T^b, u_L)$ and $R = (s_R, T^b, u_R)$. In this Riemann Problem, there are two relevant bifurcation curves. The first bifurcation occurs at the points where the thermal rarefaction speed λ_T^g (Eq. (4.9.a)) equals the shock speed v^{CS} (Eq. (5.18)). The other bifurcation appears at the points where the speed v^{CS} coincides with the Buckley-Leverett rarefaction speed λ_s^b (Eq. (4.18)) in the br .

Moreover, there is a point where all previous speeds coincide. It is a double bifurcation point in the $\{T^-; s_w^+\}$ plane of left state temperatures T^- in sr and right saturation s_w^+ in br (see Sec. 6.4.1). This point is denoted by $(\hat{T}; s^\dagger)$ and it should be understood as the projection of $(s_w = 0, \hat{T}; s^\dagger, T^b)$ onto the $\{T^-; s_w^+\}$ plane.

6.4.1. Definition of \hat{T} and s^\dagger . Let $\Upsilon = \Upsilon(T^-; s_w^+)$ be defined as:

$$\Upsilon = \frac{\rho_g^- c_g^-}{\hat{C}_r + \rho_g^- c_g^-} - \left(\frac{u^+}{u^-} \right) \frac{f_w^+ - f_w^{CS}}{s_w^+ - s_w^{CS}}. \tag{6.17}$$

The fraction u^+/u^- is obtained from Eq. (5.15). This fraction does not depend on u^- or u^+ , showing that also Υ does not depend on u^- (or u^+). Moreover, at the points $(T^-; s_w^+)$ where $\Upsilon = 0$, the equality $\lambda_T^g = v^{CS}$ holds.

Now we can define the thermal coincidence as the curve where the left thermal wave speed λ_T^g coincides with the condensation shock v^{CS} ; it is denoted by TCS locus:

$$TCS = \{(T, s) \mid \Upsilon(T, s) = 0, \text{ for } T \in sr \text{ and } s \in br\}. \tag{6.18}$$

Analogously, we define $\Lambda = \Lambda(T^-; s_w^+)$ as:

$$\Lambda = \frac{f_w^+ - f_w^{CS}}{s_w^+ - s_w^{CS}} - \frac{\partial f_w^b}{\partial s_w}, \tag{6.19}$$

where f_w^{CS} and s_w^{CS} depend on T^- , see (5.14). Now we can define the CSS locus as the curve where $v^{CS} = \lambda_s^b$ and for each T^- fixed, $v^{CS}(T^-; s_w^+)$ is understood as a function of s_w^+ that is minimized (see Prop. 6.4) :

$$CSS = \{(T^-; s_w^+) \mid \Lambda = 0 \mid v^{CS} \text{ is minimum; } T^- \in sr, s_w^+ \in br\}. \tag{6.20}$$

In Fig. 6.2, the TCS and CSS loci are shown as curves in the plane $\{T, s\}$. The horizontal axis represents the states in the sr and the vertical axis represents the states in the br . The two loci intersect transversally at $(\hat{T}; s^\dagger)$, the double bifurcation point ‘‘SHB’’. It can be obtained numerically using root finders. The temperature \hat{T} satisfies $T^b < \hat{T}$, and the saturation s^\dagger satisfies $0 < s^\dagger < 1$.

For the Riemann solution, we need to study the relationships between T_L and \hat{T} at $(s_w = 0, T^-)$, and between s_R and s^\dagger at (s_w^+, T^b) .

Defining $\Xi(T^-; s_w^+) = (f_w^+ - f_w^{CS}) / (s_w^+ - s_w^{CS})$, the *CSS* locus is obtained using the following proposition:

PROPOSITION 6.4. *There are always two water saturation values satisfying $\Lambda(T, s) = 0$ for each fixed $T > T^b$. The smallest value minimizes Ξ (and consequently v^{CS}), while the other value maximizes Ξ (and v^{CS}). We define s^\bullet as the smaller water saturation value.*

From Prop. 6.4, one can prove:

COROLLARY 6.3. *For each fixed T in the br , the solution after s^\bullet continues as a rarefaction in the br .*

Prop. 6.4 implies that for each fixed temperature T^- there are two saturations that satisfy $\Lambda = 0$, i.e. $\lambda_s^b = v^{CS}$, but we choose the one that belongs to the CSS and denote it by s^* (see [8], where this selection criterion is shown to be the Oleinik entropy condition).

In Fig. 6.3.a, we obtain the water saturation s^* , for each T^- . We represent this map of T^- into s^* , which is used in Item (2) of the following proposition, as:

$$s^* := s^*(T^-). \tag{6.21}$$

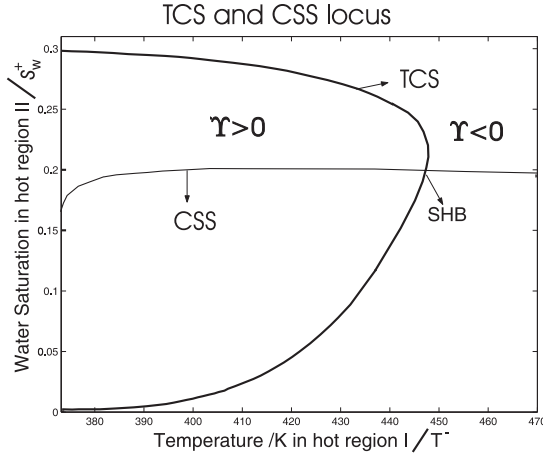


FIG. 6.2. Schematic phase space. The intersection of the TCS and CSS loci is the SHB at $(\hat{T}; s^\dagger)$. The horizontal axis represents the sr and the vertical axis represents the br , so SHB represents two points: \hat{T} is the projection of $(s_w = 0; \hat{T})$ on the sr ; s^\dagger is the projection of $(s_w = s^\dagger; T^b)$ on the br ; between the TCS locus and the water saturation axis $\Upsilon > 0$, so $\lambda_T^g > v^{CS}$; in the complementary region $\lambda_T^g < v^{CS}$.

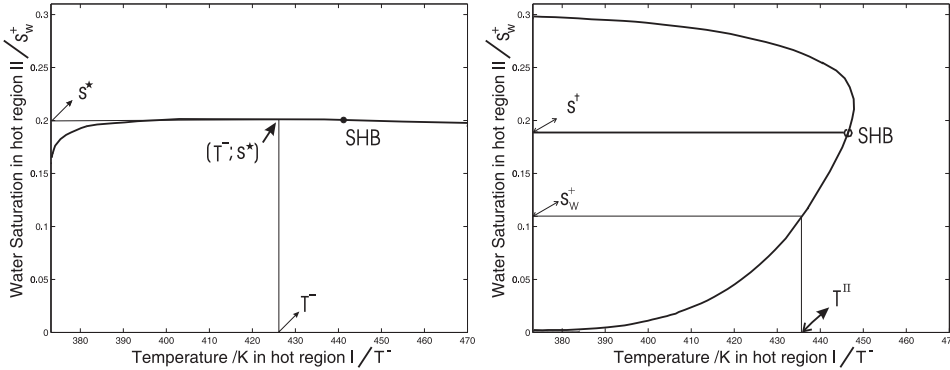


FIG. 6.3. a) Left: The graph of $\Lambda = 0$. For each T^- , the vertical line crosses the graph at a saturation $s^* = s^*(T^-)$. b)-Right: The value $T^{II}(s_R)$ is obtained from the TCS locus. We plot a horizontal line from s_w^+ , the point where this line intersects the graph Υ is the point $(T^{II}(s_w^+), s_w^+)$.

PROPOSITION 6.5. If $T^- < \hat{T}$, then $\lambda_T^g > v^{CS}$. Thus there is a shock between $(s_w = 0, T^-, u^-)$ to (s^*, T^b, u^+) . Furthermore, the solution continues in the br as a rarefaction.

Proof. The proof consist of two steps:

(1) The characteristic speed λ_T^g is larger than the shock speed v^{CS} at (T_L, s^*) . From Figs. 6.3.a and 6.2, we can see that $\Upsilon > 0$ at (T^-, s^*) , so $\lambda_T^g > v^{CS}$. Thus there is a shock between $(0, T^-, u^-)$ and (s^*, T^b, u^+) .

(2) The solution continues as a rarefaction in the br . As s^* satisfies $\Lambda = 0$, this fact follows from Cor. 6.3. \square

Prop. 6.5 yields:

COROLLARY 6.4. When T^- tends to T^b , the saturation s^* tends to s_{wc} , the

connate water saturation (see Appendix A); thus the solution is continuous when T tends to T^b between the sr and the br .

REMARK 6.2. When $T^- = T^b$, the left state lies in the br . This solution was obtained in [2]. In that case, there was a region with connate water saturation in the br . From Cor. 6.4, our solution agrees with that in [2]. Notice that the connate water in this region is immobile, but this water evaporates when the vaporization shock advances.

Fix $s_w^+ < s^\dagger$. Using the TCS locus, we obtain $T^\Pi(s_w^+)$ as a function of s_w^+ . For each s_w^+ we draw a horizontal line. We project the intersection of this horizontal line and the TCS onto the horizontal axis to obtain T^Π ; we denote this mapping by:

$$T^\Pi := T^\Pi(s_w^+). \tag{6.22}$$

It is important that $T^\Pi(s_w^+)$ is monotone for $s_w^+ < s^\dagger$.

PROPOSITION 6.6. For $s_w^+ < s^\dagger$ and $T^- > \hat{T}$, there is a rarefaction from $(0, T^-, u^-)$ to $(0, T^\Pi, u^\Pi)$. At $(0, T^\Pi, u^\Pi)$ the following speeds coincide:

$$\lambda_T^g(T^\Pi, u^\Pi) = v^{CS}(T^\Pi, u^\Pi; s_w^+), \tag{6.23}$$

so there is a left characteristic shock between $(0, T^\Pi, u^\Pi)$ and (s_w^+, T^b, u^+) with speed v^{CS} .

Proof. In Fig. 6.3.b, we plot an example of s_w^+ and its respective $T^\Pi(s_w^+)$. Since the temperature decreases from left to right along the thermal rarefaction wave, from Rem. (4.1), this wave is a rarefaction. \square

COROLLARY 6.5. When s_w^+ tends to 0 in br , the temperature T^Π converges to T^b ; thus the solution is continuous between the br and the sr .

In Eq. (6.22), we find $s^* = s^*(T^-)$; also $T^\Pi = T^\Pi(s_w^+)$ from Eq. (6.21), see Fig. 6.3.b. Using s^* and T^Π , four possible solution candidates arise:

- (i) $T^- < T^\Pi$, $s^* < s_w^-$. A shock from $(0, T^-, u^-)$ to (s^*, T^b, u^+) , continuing to (s_w^+, T^b, u^+) through a Buckley-Leverett rarefaction.
- (ii) $T^- < T^\Pi$, $s^* > s_w^+$. A shock from $(0, T^-, u^-)$ to (s_w^+, T^b, u^+) with speed v^{CS} .
- (iii) $T^- > T^\Pi$, $s^* < s_w^+$. A rarefaction from $(0, T^-, u^-)$ to $(0, T^\Pi, u^\Pi)$ followed by a shock to (s^*, T^b, u^+) continuing to (s_w^+, T^b, u^+) through a Buckley-Leverett rarefaction.
- (iv) $T^- > T^\Pi$, $s^* > s_w^+$. A rarefaction from $(0, T^-, u^-)$ to $(0, T^\Pi, u^\Pi)$, followed by a shock to (s^*, T^b, u^+) with speed v^{CS} .

PROPOSITION 6.7. For left temperature T^- and fixed right saturation s_w^+ satisfying $T^- < \hat{T}$ and $s_w^+ < s^\dagger$, (i) and (iii) do not occur.

Proof. From Fig. 6.4.a, we separate the water saturation in the br (the right side states of the Riemann problem) in two intervals, s_{RegI} and s_{RegII} . The first one is $s_w^+ \in [s_{wc}, s^\dagger,]$; the second one is $s_w^+ \in [s_w = 0, s_{wc}]$. Recall Eq. (6.22), which defines T^Π as function of s_w^+ . So we define $T_{RegI} = T^\Pi(s_{RegI})$; similarly, we define $T_{RegII} = T^\Pi(s_{RegII})$. One can verify from Fig. 6.4.a that $T^\Pi(s_w^+)$ is monotone increasing.

Fig. 6.4.b represents the mapping from T_{RegI} to the br . Each value of $T^- \in T_{RegI}$ defines a value for s^* in the br through the function $s^*(T^-)$ in Eq. (6.21). The function

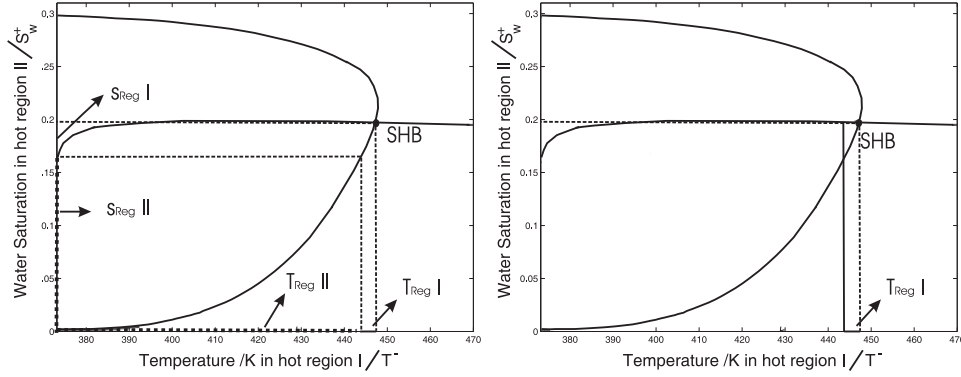


FIG. 6.4. a)-Left: The map T^{II} defines $T_{\text{Reg I}}$ and $T_{\text{Reg II}}$. The saturation lies in the br, which is subdivided in $s_{\text{Reg I}} = [s_{wc}, s^\dagger]$ and in $s_{\text{Reg II}} = [0, s_{wc}]$. The corresponding intervals in the sr are $T_{\text{Reg I}}$ and $T_{\text{Reg II}}$. b)-Right: Mapping from $T_{\text{Reg I}}$ to br. Each $T^- \in T_{\text{Reg I}}$ defines a s^* in the br (see Prop. 6.6); notice that s^* satisfies $s^* \geq s^\dagger$, which is the saturation at SHB.

$s^*(T^-)$ is not monotone and all values of $s^* = s^*(T^-)$ for $T^- \in T_{\text{Reg I}}$ are larger or equal to s^\dagger , the saturation at the SHB point. Notice also that the mapping $s^*(T^-)$ for $T^- \in T_{\text{Reg I}} \cup T_{\text{Reg II}}$ is onto $s_{\text{Reg I}}$. So we obtain that $s_w^+ < s^*(T^-)$ for $T^- \in T_{\text{Reg I}}$, so (i) and (iii) do not occur. \square

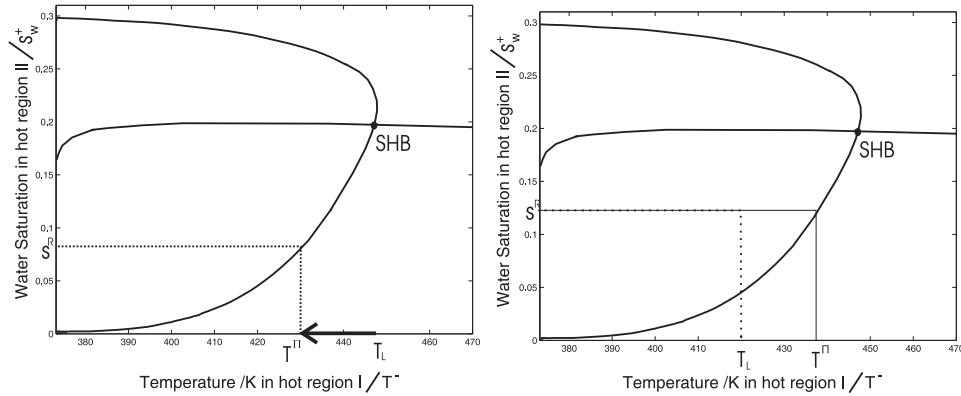


FIG. 6.5. a)-Left: Riemann Solution. the point T_L in the horizontal axis represents $(s_L = 0, T_L)$. The rarefaction from $(s_L = 0, T_L)$ to $(s_L = 0, T^{\text{II}})$ is represented by a line and an arrow to indicate the direction of increasing speed; the rarefaction is followed by a shock from $(s_w = 0, T^{\text{II}})$ to (s_R, T^b) with speed v^{CS} with construction shown by dotted lines. b)-Right: the dotted line represents the shock from $(s_L = 0, T_L, u_L)$ to (s_R, T^b, u_R) with speed v^{CS} . We draw the solution for a left state $(s_L = 0, T_L)$, which we represent by T_L .

Solution: (summarized in Fig 6.6).

(I) For $T_L > \hat{T}$ and $s_R > s^{\text{infl}} > s^\dagger$. The waves $R_T \rightarrow CS \rightarrow R_s \rightarrow S_s$ with sequence:

$$L = (0, T_L, u_L) \xrightarrow{R_T} (0, \hat{T}, \hat{u}) \xrightarrow{CS} (s^\dagger, T^b, u_R) \xrightarrow{R_s} (s^\S, T^b, u_R) \xrightarrow{S_s} (s_R, T^b, u_R) = R, \tag{6.24}$$

where (\hat{T}, s^\dagger) is the SHB point and s^\S is given by Eq. (6.12).

(II) For $T_L > \hat{T}$ and $s^{infl} > s_R > s^\dagger$. The waves $R_T \rightarrow CS \rightarrow R_s$ with sequence:

$$L = (0, T_L, u_L) \xrightarrow{R_T} (0, \hat{T}, \hat{u}) \xrightarrow{CS} (s^\dagger, T^b, u_R) \xrightarrow{R_s} (s_R, T^b, u_R) = R. \quad (6.25)$$

(III) For $T^\Pi < T_L$ and $s_R < s^*(T_L)$. The solution is sketched in Fig. 6.5.a, based on Props. 6.7 and 6.6; the waves are $R_T \rightarrow CS$ with sequence:

$$L = (0, T_L, u_L) \xrightarrow{R_T} (0, T^\Pi < \hat{T}, u^\Pi) \xrightarrow{CS} (s_R, T^b, u_R) = R. \quad \square \quad (6.26)$$

(IV) For $T^\Pi > T_L$ and $s_R < s^*(T_L)$, the solution is sketched in Fig. 6.5.b. It is the wave CS with sequence:

$$L = (0, T_L, u_L) \xrightarrow{CS} (s_R, T^b, u_R) = R. \quad (6.27)$$

(V) For $T_L < \hat{T}$ and $s^{infl} > s_R > s^*(T_L)$, where the mapping $s^* = s^*(T_L)$ is defined in Eq. (6.21). We obtain the waves $CS \rightarrow R_s$ with sequence:

$$L = (0, T_L, u_L) \xrightarrow{CS} (s^*, T^b, u_R) \xrightarrow{R_s} (s_R, T^b, u_R) = R. \quad (6.28)$$

(VI) For $T_L < \hat{T}$ and $s_R > s^{infl} > s^\dagger$. See (6.28). The waves $CS \rightarrow R_s \rightarrow S_s$ with sequence:

$$L = (0, T_L, u_L) \xrightarrow{CS} (s^*, T^b, u_R) \xrightarrow{R_s} (s^\S, T^b, u_R) \xrightarrow{S_s} (s_R, T^b, u_R) = R, \quad (6.29)$$

where s^\S is given by Eq. (6.12) with $s_w^+ = s_R$.

REMARK 6.3. We remark that the CS is a double sonic transitional wave, see [10].

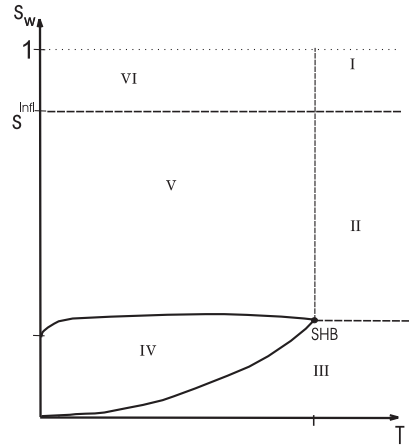


FIG. 6.6. Phase diagram for Riemann Problem C. The dotted line delimits the physical range, the dashed lines are bifurcation loci. The continuous curves are parts of the TCS and the CSS bifurcations loci. The horizontal axis represents the left states $(0, T_L, u_L)$ in sr ; the vertical axis represents the right states (s_R, T^b, u_R) in br . The solutions are given in I-VI, Sec. 6.4.

6.5. Riemann Problem D. We inject pure water at temperature $T_L < T^b$, i.e, the left state is $(1, T_L, u_L)$; on the right we have pure steam at temperature $T_R > T^b$.

Before describing our proposed Riemann solution, it is necessary to prove that there is no possible Riemann solution with a direct shock between sr and the wr . Using the RH condition (5.4)-(5.5) with $s_w^+ = 0$ and T^b replaced by $T^+ > T^b$, we obtain this hypothetical “complete water evaporation shock”, labelled $CWES$, with speed v^{CWES} . The superscript $+$ ($-$) in the following equations represents the temperature T^+ (T^-). The speed of such shock between $(s_w = 1, T^-, u^w)$ to $(s_w = 0, T^+ > T^b, u)$ would be:

$$v^{CWES}(T^-, u^-; s_w^+ = 0, T^+) = \frac{u^w}{\varphi} \frac{\rho_w(h_g^+ - h_w^-)}{H_r^+ - H_r^- + \rho_w(h_g^+ - h_w^-)}. \quad (6.30)$$

PROPOSITION 6.8. *Complete Evaporation.* For any $T^- < T^b < T^+$, if there exists a complete water evaporation shock from $(1, T^-, u^-)$ to $(0, T^+ > T^b, u^+)$ with speed $v^{CWES}(T^-, u^-; s_w^+ = 0, T^+)$ given by (6.30), then this shock satisfies:

$$v^{CWES} > v_T^w, \quad (6.31)$$

where v_T^w is the speed of thermal discontinuity given by Eq. (4.20).

If this shock exists, it would not satisfy the Oleinik condition for entropy [9]. Therefore we conclude that instead of a shock there is a br between the $(-)$ and $(+)$ state. The solution is constructed using results from Sections 6.2 and 6.3. Since $s_w^+ = 0$, from Sec. 6.3 we obtain:

PROPOSITION 6.9. *The saturation $s_{\dagger\dagger}$ in (6.11) is larger than \hat{s} (defined in (6.5)), thus there is a rarefaction from $(s_{\dagger\dagger}, T^b, u^+)$ to (\hat{s}, T^b, u^+) .*

Solution. The solution consists of the waves $WES \rightarrow R_s \rightarrow CS$ with sequence:

$$L = (1, T_L, u_L) \xrightarrow{WES} (s_{\dagger\dagger}, T^b, u_R) \xrightarrow{R_s} (\hat{s}, T^b, u_R) \xrightarrow{SC} (0, T_R, u_R) = R. \quad (6.32)$$

6.6. Riemann Problem E. We inject pure steam at temperature $T_L > T^b$, i.e, $L = (0, T_L > T^b, u_L)$; on right we have pure water at $T_R < T^b$, i.e., the right state is $R = (1, T_R < T^b, u_R)$. We use results from Section 6.5 to obtain the solution.

We remark that the vaporization shock, VS, is the reverse of the condensation shock, CS, so there could exist a hypothetical “complete condensation shock”, labelled CCS , with speed v^{CCS} . This shock would be obtained using the RH condition (5.11)-(5.12) with the $(-)$ state replaced by $(s_w = 1, T^+ < T^b, u^+)$, and the $(+)$ state replaced by $(s_w^- = 0, T^- > T^b, u^-)$. The speed of such shock would be:

$$v^{CCS}(T^-, u^-; s_w^+ = 1, T^+) = \frac{u^-}{\varphi} \frac{\rho_g^-(h_g^+ - h_w^-)}{H_r^+ - H_r^- + \rho_g^+(h_g^+ - h_w^-)}. \quad (6.33)$$

The following fact indicates that instead of this shock, there is always a br between the sr and the wr .

PROPOSITION 6.10. *Complete Condensation.* For any $T^- \geq T^b$ the complete condensation shock from $(s_w = 0, T^-, u^-)$ to $(s_w = 1, T^+, u^+)$ with speed $v^{CCS}(T^-, u^-; s_w^+ = 1)$ satisfies:

$$v^{CCS} > \lambda_T^g(T^-, u^-). \quad (6.34)$$

The inequality (6.34) in Prop. 6.10 shows that there is a br between $(s_w = 0, T^-, u^-)$ and $(s_w = 1, T^+, u^+)$. In [2], Bruining et al. obtained the solution for injection of water and steam at boiling temperature in a porous rock filled with water. In that work, the water and rock enthalpies were made to vanish at a certain temperature T^0 . In the current work we do not use T^0 , so the formulae for shock speeds appear to be slightly different from formulae in [2]; however, both are equivalent since the enthalpy is defined in up to a constant. In that paper, two saturations denoted by s_{\dagger} and s_{\ddagger} were found both satisfying Eq. (6.11); the choice for s_{\ddagger} was also made.

To complete the Riemann solution, we obtain a relationship between s^* and s^{\dagger} :

PROPOSITION 6.11. *The water saturation s^* , defined in (6.21), obtained in the br by a shock from $(0, T^-, u^-)$ to (s^*, T^b, u^+) satisfies the following inequality:*

$$s^* < s_{\dagger},$$

so from (s^*, T^b, u^+) the solution continues as a rarefaction to (s_{\dagger}, T^b, u^+) .

Solution. We obtain the Riemann solution using the results in [2], [5] and (6.29), (6.24).

For $T_L < \hat{T}$. As in (6.29), there is a shock from $L = (0, T^-, u^-)$ to (s^*, T^b, u^+) where $s^* = s^*(T_L)$ is given by (6.21) and s_{\dagger} satisfies Eq. (6.11). The waves are $CS \rightarrow R_s \rightarrow SCF$ with sequence:

$$L = (0, T_L, u_L) \xrightarrow{CS} (s^*, T^b, u_R) \xrightarrow{R_s} (s_{\dagger}, T^b, u_R) \xrightarrow{SCF} (s_R, T^b, u_R) = R. \quad (6.35)$$

For $T_L > \hat{T}$. The waves $R_T \rightarrow CS \rightarrow R_s \rightarrow SCF$ with sequence:

$$L = (0, T_L, u) \xrightarrow{R_T} (0, \hat{T}, u) \xrightarrow{CS} (s^{\dagger}, T^b, u^b) \xrightarrow{R_s} (s_{\dagger}, T^b, u^b) \xrightarrow{SCF} (s, T < T^b, u_R) = R, \quad (6.36)$$

where (\hat{T}, s^{\dagger}) is the SHB point.

7. Summary and Conclusions. We have described completely all possible solutions of the Riemann problem for the injection of a mixture of steam and water in several proportions and temperature into a porous rock filled with a different mixture of steam and water in all proportions, (of course, the temperature must be lower than the thermodynamical critical temperature of water). The set of solutions depends L^1 continuously on the Riemann data.

We found several types of shock between regions and systematized a scheme to find the solution from these shocks. A new type of shock, the evaporation shock, was identified. This work generalizes [2] of Bruining et al. It is a step towards obtaining a general method for solving Riemann problems for a wide class of balance equations with phase changes (see [8]).

REFERENCES

- [1] BAYLISS, A., MATKOWSKY, B. J, AND ALDUSHIN, A. P., *Dynamics of hot spots in solid fuel combustion*, Physica D, 166:1-2 (2002), pp. 104–130.
- [2] BRUINING, J., MARCHESIN, D. E VAN DULJN, C. J., *Steam Injection Into Water-Saturated Porous Rock*, Computational and Applied Mathematics, 22:3 (2003), pp. 359-395.
- [3] KULIKOVSKII, A. G., *Evaporation and Condensation Front in Porous Media*, Fluid Dynamics, 37:5 (2002), pp. 740–746, 2002.

- [4] E. ISAACSON, MARCHESIN, D., PLOHR, B., AND TEMPLE, J., B., *Multiphase flow models with singular Riemann problems*, Mat. Apl. Comput., 11:2 (1992), pp. 147–166.
- [5] LAMBERT, W., BRUINING, J. AND MARCHESIN, D., *Erratum: Steam Injection Into Water-Saturated Porous Rock*, to appear in Computational and Applied Mathematics, 2006.
- [6] LAMBERT, W., MARCHESIN, D., BRUINING, J. AND ALBUQUERQUE, D., *Numerical method for nitrogen and steam injection into porous medium with water*, Rio Oil Gas 2004, available in CD-ROM.
- [7] LAMBERT, W., MARCHESIN, D. AND BRUINING, J., *The Riemann Solution of the Balance Equations for Steam and Water Flow in a Porous Medium*, preprint IMPA-A426, available at <http://www.preprint.impa.br>, pp. 1–41, (2006).
- [8] LAMBERT, W. *Doctoral Thesis: IMPA*, 2006, in preparation.
- [9] OLEINIK, O., *Discontinuous Solutions of Nonlinear Differential Equations* Usp. Mat. Nauk. (N. S.), 12 (1957), pp. 3–73. English transl. in Amer. Math. Soc. Transl. Ser., 2, 26, pp. 95–172.
- [10] SCHECTER, S., PLOHR, B. AND MARCHESIN, D., *Classification of Codimension-One Riemann Solutions*, Journal of Dynamics and Differential Equations, 13:3 (2001), pp. 523–588.
- [11] SMOLLER, J., *Shock Waves and Reaction-Diffusion Equations*, Springer-Verlag, 1983.
- [12] TSYPKIN, G.G. AND WOODS, A. W. *Vapour extraction from a water-saturated geothermal reservoir*, J. Fluid Mech., 506 (2004), pp. 315–330, Cambridge University Press.

Appendix A. Physical quantities; symbols and values.

A.1. Temperature dependent properties of steam and water. We use reference [1] to obtain all the temperature dependent properties below. The water and steam densities used to obtain the enthalpies are defined at the bottom.

The steam enthalpy h_g [J/kg] as a function of temperature is approximated by

$$h_g = -2.20269 \times 10^7 + 3.65317 \times 10^5 T - 2.25837 \times 10^3 T^2 + 7.3742 T^3 - 1.33437 \times 10^{-2} T^4 + 1.26913 \times 10^{-5} T^5 - 4.9688 \times 10^{-9} T^6. \quad (\text{A.1})$$

We also use the temperature dependent steam viscosity

$$\mu_g = -5.46807 \times 10^{-4} + 6.89490 \times 10^{-6} T - 3.39999 \times 10^{-8} T^2 + 8.29842 \times 10^{-11} T^3 - 9.97060 \times 10^{-14} T^4 + 4.71914 \times 10^{-17} T^5. \quad (\text{A.2})$$

The temperature dependent water viscosity μ_w is approximated by

$$\mu_w = -0.0123274 + \frac{27.1038}{T} - \frac{23527.5}{T^2} + \frac{1.01425 \times 10^7}{T^3} - \frac{2.17342 \times 10^9}{T^4} + \frac{1.86935 \times 10^{11}}{T^5}. \quad (\text{A.3})$$

We assume that the steam is a ideal gas, so the steam density is a function of temperature:

$$\rho_g(T) = p \frac{M_{H_2O}}{R} \frac{1}{T}, \quad (\text{A.4})$$

where M_{H_2O} is the water molecular mass [Kg/m^3], p is the pressure atmospheric [Pa] and $R=8.31$ [J/mol K]. The quantity pM_{H_2O}/R is a constant.

The liquid water density is constant, and the value is $998.2 \text{Kg}/\text{m}^3$.

We define \hat{H}_r and the water enthalpy per mass unit h_w respectively as:

$$\hat{H}_r(T) = (1 - \varphi)/\varphi C_r T \quad \text{and} \quad h_w = C_w T / \rho_w. \quad (\text{A.5})$$

A.2. Constitutive relations. The relative permeability functions k_{rg} and k_{rw} are considered to be power functions of their respective saturations *i.e.*

$$k_{rg} = \left(\frac{s_g}{1 - s_{wc}} \right)^{n_g} \quad \text{and} \quad k_{rw} = \begin{cases} \left(\frac{s_w - s_{wc}}{1 - s_{wc}} \right)^{n_w} & \text{for } s_w \geq s_{wc}, \\ 0 & \text{for } 0 \leq s_w \leq s_{wc}, \end{cases} \quad . \quad (\text{A.6})$$

For the computations we take $n_w = 4$, $n_g = 2$. The connate water saturation s_{wc} is given in Table 2 below.

Table 2, Summary of physical input parameters and variables			
<i>Physical quantity</i>	<i>Symbol</i>	<i>Value</i>	<i>Unit</i>
Water, steam fractional functions	f_w, f_g	Eq. (2.5) .	$[\text{m}^3/\text{m}^3]$
Porous rock permeability	k	1.0×10^{-12} .	$[\text{m}^3]$
Water, steam relative permeabilities	k_{rw}, k_{rg}	Eq. (A.6) .	$[\text{m}^3/\text{m}^3]$
Pressure	p	1.0135×10^5 .	[Pa]
Mass condensation rate	q	Eqs (2.1)-(2.2).	$[\text{kg}/(\text{m}^3\text{s})]$
Water, steam phase velocity	u_w, u_g	Eq. (2.4) .	$[\text{m}^3/(\text{m}^2\text{s})]$
Total Darcy velocity	u	$u_w + u_g$, Eq (2.6).	$[\text{m}^3/(\text{m}^2\text{s})]$
Water and rock heat capacity	C_w, C_r	$4.22 \times 10^6, 2.029 \times 10^6$.	$[\text{J}/(\text{m}^3\text{K})]$
Steam and water enthalpies	h_g, h_w	Eqs. (A.1), (A.5.b).	$[\text{J}/\text{m}^3]$
Rock enthalpy	H_r	$(1 - \varphi)C_r T$.	$[\text{J}/\text{m}^3]$
Water, steam saturations	s_w, s_g	Dependent variables.	$[\text{m}^3/\text{m}^3]$
Connate water saturation	s_{wc}	0.15.	$[\text{m}^3/\text{m}^3]$
Temperature	T	Dependent variable.	[K]
Boiling point of water–steam	T^b	$\simeq 373.15$.	[K]
Water, steam thermal conductivity	κ_w, κ_g	0.652, 0.0208.	$[\text{W}/(\text{mK})]$
Rock, composite thermal conductivity	κ_r, κ	1.83 .	$[\text{W}/(\text{mK})]$
Water, steam viscosity	μ_w, μ_g	Eqs. (A.3) , (A.2).	$[\text{Pa s}]$
Water, steam densities	ρ_w, ρ_g	998.2, Eq. (A.4) .	$[\text{kg}/\text{m}^3]$
Rock porosity (constant)	φ	0.38.	$[\text{m}^3/\text{m}^3]$